

Design of Inflow-Adapted Foil Sections by Using a Multi-Objective Optimization Method

Jeng-Lih Hwang¹, Ching-Yeh Hsin², Yu-Hua Cheng², Shang-Sheng Chin²

¹United Ship Design and Development Center (USDDC), Taipei, Taiwan

²Department of Systems Engineering and Naval Architecture, National Taiwan Ocean University, Keelung, Taiwan

ABSTRACT

In this paper, a design procedure for designing the inflow-adapted foil sections is presented. The design goal is to design a foil section not only having a satisfactory performance, but also having consistent performance at different design conditions, for example, different speeds or different angles of attack. We define foils designed based on this design goal as an “inflow-adapted” foil. Three design algorithms are described in the paper, and they are design a foil based on the given pressure distribution, single objective optimization based on the Lagrange Multiplier method and an extended multi-objective optimization method. A viscous flow RANS method is used for the computation, and the cavitation is also considered in the computations. The optimization problem described in the paper is to satisfy the lift requirement by minimizing the drag force, and design examples of single objective are shown in the paper. A multi-objective inflow-adapted foil design is also presented. All the design cases show that the design method presented in this paper is effective. The foil sections designed based on the presented procedure are expected to be used on propellers operated in a large range of speeds or with the inclined shaft.

Keywords

Foil design, multi-objective optimization, Lagrange Multiplier method, RANS

1 INTRODUCTION

Two-dimensional foil designs have been widely applied to different applications, such as marine propellers, rudders, pumps, wind turbines, cooling fans, etc., and many newly-designed foil geometries have been successfully applied to the performance improvements for different purposes. In the marine propeller applications, two-dimensional foil sections, such as NACA series, Newton-Rader sections, Eppler sections have been used for different design considerations. In this paper, a design procedure for designing the inflow-adapted foil sections is presented. The “inflow-adapted” foil section is defined as a foil section not only having a satisfactory performance, but also having consistent performance at

different design conditions, for example, different speeds or different angles of attack.

The foil design problem was first studied by Lighthill (Lighthill 1945), and he solved it for the case of the incompressible flow by using the conformal mapping technique. Since then, many methods have been developed (Tranen 1974) (Henne 1985) (Volpe 1986), and most of these methods mapped the foil shape to a mapping plane. Eppler (1980), Giles (1986) and Drela (1989) developed methods extensively used by the industry. Eppler's sections are famous for its advantages in the prevention of cavitations. Drela and Giles developed a method based on the boundary element method with the incorporation of the boundary layer computations, and this method is then developed as the widely used foil design tool XFOIL. The Genetic Algorithms and the Evolutionary Strategy are also used for the foil designs, such as De Falco (1997) and Obayashi (1995). Hsin(1994, 1998, 2000) has developed a method to design a foil based on the given pressure distribution. That is, a pressure distribution is given, and the foil geometry is directly obtained in the Cartesian coordinate system by solving the Laplace's equation. The pressure distribution has to satisfy certain physical constraints such as existence of the stagnation point, satisfaction of the Kutta condition, etc. An optimization method using the Lagrange Multiplier method is later developed to improve the design procedure (Wu, 2005), and the performance of the foil thus can be optimized. In this paper, a simple multi-objective method also based on the Lagrange Multiplier method is presented, and different design algorithms are integrated to design the inflow-adapted foil sections.

2 DESIGN ALGORITHMS

In order to satisfy different design purposes, three foil design algorithms are developed and integrated. We will introduce these algorithms in this section, and they are:

- (1) Design a foil based on the given pressure distribution,
- (2) Optimize the foil performance based on the Lagrange Multiplier method,
- (3) Multi-objective optimization.

2.1 Design based on the given pressure distribution

In this algorithm, the foil geometry is defined by B-splines:

$$x(t) = \sum_{i=1}^{N_v} (x_v)_i B_i^4(t) \quad y(t) = \sum_{i=1}^{N_v} (y_v)_i B_i^4(t) \quad (1)$$

where t is the B-splines parameter, x_v and y_v are control points, N_v is the number of control points, and B_i^4 is the B-splines basis functions of order 4 (degree 3). To design a foil based on a prescribed pressure distribution, the Newton-Raphson method is used. The designed foil geometry can thus generate the prescribed pressure distribution. Different kinds of computational methods can be used for the flow computations, such as potential flow boundary element method or the viscous flow RANS method.

Since the foil geometry is defined by B-splines, and the pressure distribution on the foil can thus be expressed as a function of B-spline control points;

$$C_p = C_p(\bar{X}) \quad (2)$$

$$\bar{X} = [(x_v, y_v)_1, (x_v, y_v)_2, (x_v, y_v)_3, \dots, (x_v, y_v)_{N_v}]$$

A Jacobian is established by relating the geometry changes and the pressure changes :

$$[J] = \left[\frac{\partial(Cp)_i}{\partial(\bar{X})_j} \right] \quad (3)$$

where $(Cp)_i$ is the pressure distribution on the i^{th} collocation point, and $(\bar{X})_j$ is the j^{th} control point.

By defining $\delta(Cp^*)$ as the difference between the designed pressure distribution and the desired pressure distribution, we can then solve a nonlinear equation

$$[\delta(Cp^*)] = 0 \quad (4)$$

by the Newton-Raphson method :

$$[\bar{X}]^{k+1} = [\bar{X}]^k - [J]^{-1}[\delta Cp^*]^k \quad (5)$$

2.2 Lagrange Multiplier Method

The design algorithm described above, although designers can specify a pressure distribution based on the desired local characteristics, it is hard to know the forces on the desired foil in advance. Therefore, an optimization method using the Lagrange Multiplier method is then developed. The Lagrange Multiplier method can transfer a constrained problem to a non-constrained problem by introducing the Lagrange multiplier λ . For example, the constrained optimization problem of the foil design problem is to find a two-dimensional foil geometry which provides the minimum drag coefficient (C_D) with a given lift coefficient (C_L). The constraint is therefore, $C_L = C_L^*$, and C_L^* is the objective lift coefficient. The design problem thus can be stated as:

$$\begin{cases} \min & C_D \\ \text{subject to} & C_L - C_L^* = 0 \end{cases} \quad (6)$$

We also assume that the lift coefficient and the drag coefficient are functions of angle of attack and geometric parameters. The geometric parameters can be defined by different ways such as camber ratio, thickness, or B-spline control points that defined the foil geometry, etc.

$$\begin{aligned} C_L &= C_L(\alpha, \gamma_i) \\ C_D &= C_D(\alpha, \gamma_i) \end{aligned} \quad i = 1, 2, 3, \dots, m \quad (7)$$

In equation (7), α is the angle of attack, and γ_i is the geometric parameters.

We thus can define the Lagrangian of this optimization problem as:

$$L = C_D + \lambda(C_L - C_L^*) \quad (8)$$

and the derivatives of equation (8) with respect to angle of attack, geometric parameters and Lagrange multiplier can be obtained:

$$\begin{aligned} \nabla_v L &= \nabla_v C_D + \lambda \nabla_v C_L = 0 \\ C_L - C_L^* &= 0 \end{aligned} \quad (9)$$

∇_v is defined as the gradient to angle of attack and geometric parameters, and $\nabla_v L$ can be expressed as

$$\begin{aligned} \frac{\partial C_D}{\partial \alpha} + \lambda \frac{\partial C_L}{\partial \alpha} \\ \frac{\partial C_D}{\partial \gamma_i} + \lambda \frac{\partial C_L}{\partial \gamma_i} \end{aligned} \quad i = 1, 2, \dots, m \quad (10)$$

This is a non-linear optimization problem, and we define:

$$G = \begin{bmatrix} \nabla_v L \\ C_L - C_L^* \end{bmatrix}, \quad \vec{X} = \begin{bmatrix} \alpha \\ \lambda \\ \vec{\gamma} \end{bmatrix} \quad (11)$$

where $\vec{\gamma} = [\gamma_1, \gamma_2, \dots, \gamma_m]^T$ if there are m geometric parameters. The solution of this optimization problem is to solve:

$$G(\vec{X}) = 0 \quad (12)$$

The Newton's method is used to solve this non-linear problem, and we can get

$$\Delta \vec{X}^j = - \frac{G(\vec{X}^j)}{\nabla G_j} \quad (13)$$

In equation (13), the update of \vec{X} is to update the angle of attack, the geometric parameters and the Lagrange multiplier. After an iterative procedure, equation (13) can be solved, and the design is reached.

2.3 Multi-objective Lagrange Multiplier Method

The Lagrange Multiplier method described above can be extended to solve a multi-objective problem by introducing a weighting function. For the cases of the "inflow-adapted" foil designs, the designed foil has to satisfy the force requirements at different conditions, for example, different speeds or different angles of attack.

Therefore, we have the following objective functions and constraints:

$$\begin{cases} \min & C_D^k \\ \text{subject to} & C_L^k - C_L^{k*} \geq 0 \end{cases} \quad k=1,2,3\dots \quad (14)$$

The index k indicates different design conditions. When optimizing the performance of a foil in different conditions, it is not easy to satisfy the same lift requirements. Therefore, usually we can only give the minimum requirements. For the following constraints:

$$C_L^k - C_L^{k*} \geq 0$$

We can use a slack variable s_k to convert the constraints to:

$$C_L^k - C_L^{k*} - s_k^2 = 0 \quad (15)$$

In order to optimize the foil performance in different conditions, we then introduce a weighting function w , and the Lagrangian of this optimization problem becomes:

$$L = \sum_{k=1}^N [w_k C_D^k + \lambda_k (C_L^k - C_L^{k*} - s_k^2)] \quad (16)$$

In equation (16), the weighting function w is given by the designers by judging the importance of each design condition. We can still follow equations (9) to (13) to solve this optimization problem except that the slack variables have also to be solved. The equation (9) and equation (11) thus become the following equations.

$$\begin{aligned} \nabla_V L &= \sum_{k=1}^N [w_k \nabla_V C_D^k + \lambda_k \nabla_V C_L^k] = 0 \\ 2\lambda_k s_k &= 0 \\ C_L^k - C_L^{k*} - s_k^2 &= 0 \end{aligned} \quad (17)$$

We can define:

$$G = \begin{bmatrix} \nabla_V L \\ 2\lambda_k s_k \\ C_L^k - C_L^{k*} - s_k^2 \end{bmatrix}, \quad \vec{X} = \begin{bmatrix} \alpha \\ \vec{\lambda} \\ \vec{\gamma} \\ \vec{s} \end{bmatrix} \quad (18)$$

where $\vec{\gamma} = [\gamma_1, \gamma_2, \dots, \gamma_m]^T$ if there are m geometric parameters, $\vec{\lambda} = [\lambda_1, \lambda_2, \dots, \lambda_N]^T$ and $\vec{s} = [s_1, s_2, \dots, s_N]^T$ if there are N constraints (N design conditions). Equations (12) and (13) are then used to solve this multi-objective optimization problem.

The multi-objective optimization algorithm described in this section is a very simple method; however, it seems to be very effective.

3 SINGLE OBJECTIVE DESIGN EXAMPLES

In this section, we will demonstrate several single objective design examples, and a multi-objective inflow-adapted foil design will be shown in the next section. From the algorithms introduced in the last section, The single objective design procedure is as the following steps:

- (1) Under the constraint that $C_L - C_L^* = 0$, computing $\frac{\partial C_D}{\partial \alpha}, \frac{\partial C_L}{\partial \alpha}, \frac{\partial C_D}{\partial \gamma}, \frac{\partial C_L}{\partial \gamma}$;
- (2) Computing elements of G and ∇G in equation (13);
- (3) Solving equation (13) to obtain $\Delta \alpha$, $\Delta \gamma$ and $\Delta \lambda$;
- (4) Updating the geometric parameter γ , angle of attack α and Lagrange multiplier λ ;
- (5) Repeating steps (1) to (4), until the equation (9) is satisfied.

The flow field computation is by a commercial viscous flow RANS method FLUENT.

3.1 Design Example 1

In the first design example, we define the geometric parameter γ as the camber ratio, and the design goal is to obtain the lift coefficient $C_L = 0.7$ with the minimum drag coefficient.

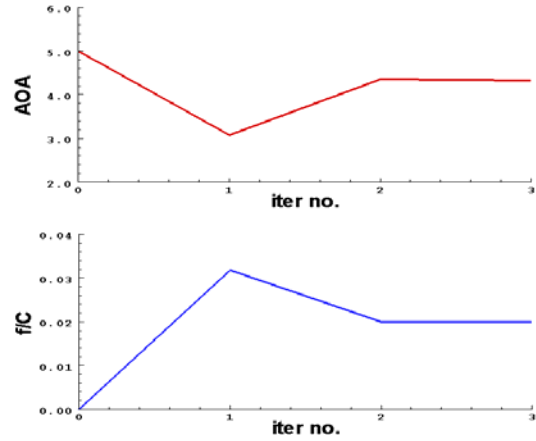


Figure 1. The convergence history of the angle of attack (AOA) and the camber ratio (f/C) of the design example 1

The initial foil geometry is a NACA 1215 section (thickness ratio is 15%, and the maximum camber is located at 20% of the foil from leading edge). Figure 1 shows the convergence history of the angle of attack (AOA) and the camber ratio (f/C), and Figure 2 shows the variations of the lift and drag coefficients during the iterations. It is obvious that the solutions are converged at the 3rd iteration. In order to verify this design, we compare our design with the performance of the NACA 0015 foil (the camber ratio is 0). Table 1 shows that the NACA 0015 section has the lift coefficient 0.7 at the angle of attack 6.249 degrees, and the drag coefficient is 0.00725. The drag is 15% higher than the designed foil. Figure 3 shows the comparison between the designed foil and NACA 0015 section, and Figure 4 shows the comparison of the pressure distributions between the designed foil and NACA 0015 section with the same lift coefficient. Note that the pressure distribution look like a “bump” near the leading edge is due to that the maximum camber distribution is located at 20% of the foil.

Table 1 Verification of the Design Example 1

	α	Camber ratio	C_L	C_D
Design	4.328	0.02	0.7	0.00612
Verification	6.249	0.00	0.7	0.00725

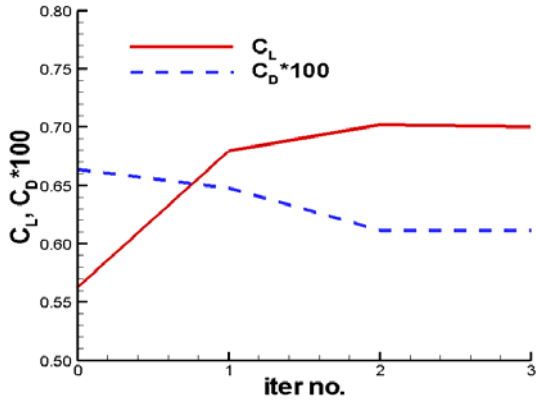


Figure 2. The variations of the lift coefficients (C_L) and drag coefficients (C_D) during the iterations of design example 1

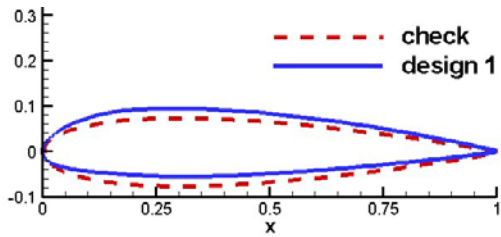


Figure 3. The designed foil geometry (design 1) of design example 1 and NACA 0015 section (check)

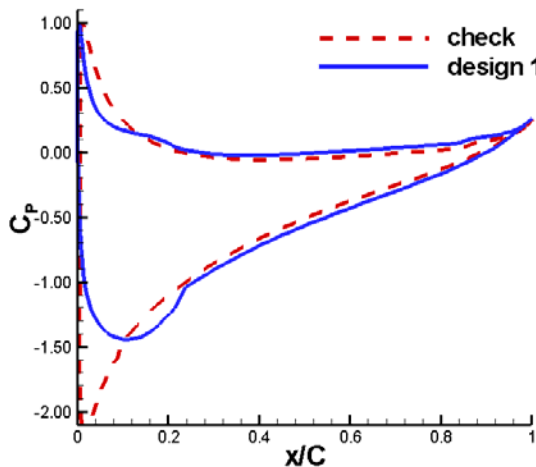


Figure 4. The pressure distributions of the designed foil (design 1) and NACA 0015 section (check) with the same lift coefficient

3.2 Design Example 2

In the design example 2, we still define the geometric parameter as the camber ratio; however, the objective lift coefficient is higher, and $C_L = 1.2$.

The NACA 1215 section is still used as the initial foil geometry, and 8 iterations are needed in this example due to the higher lift coefficient. In order to verify this design, we compare our design with the performance of the NACA 0015 foil. Table 2 shows that the NACA 0015 section with the lift coefficient 1.2. The angle of attack is 10.904 degrees, and the drag coefficient is 0.01076. The drag is almost 30% higher than that of the designed foil. Figure 5 shows the comparison between the designed foil and NACA 0015 section, and Figure 6 shows the comparison of the pressure distributions between the designed foil and NACA 0015 section with the same lift coefficient. One can see that the pressure distribution is very similar to that of the design example 1, and the camber ratio of the designed foil is obviously larger than that of the design example 1.

Table 2 Verification of the Design Example 2

	α	Camber ratio	C_L	C_D
Design	6.846	0.0396	1.2	0.00753
Verification	10.904	0.0	1.2	0.01076

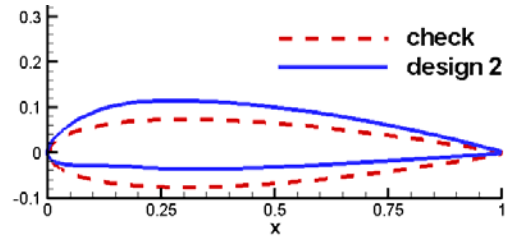


Figure 5. The comparison between the designed foil (design 2) and NACA 0015 section (check)

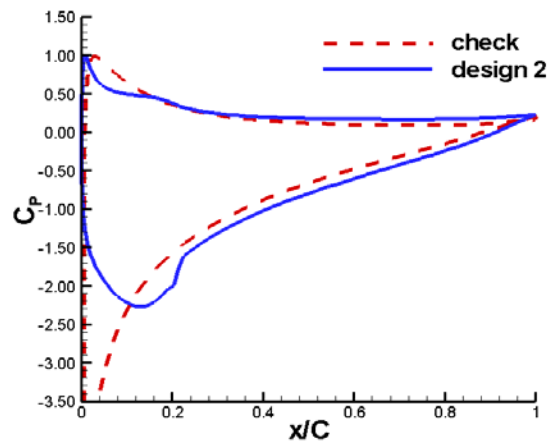


Figure 6. The pressure distributions of the designed foil (design 2) and NACA 0015 section (check) with the same lift coefficient

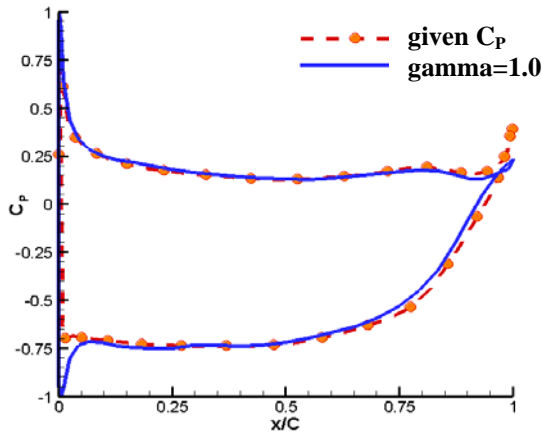


Figure 7. The given pressure distribution “shape function”, and the designed pressure distribution corresponding to $\gamma = 1.0$

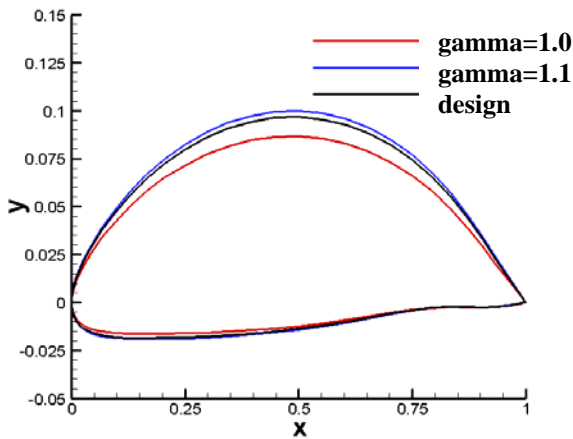


Figure 8. The designed foil geometry and foil geometries corresponding to the geometric parameters $\gamma = 1.0$ and $\gamma = 1.1$ in design example 3

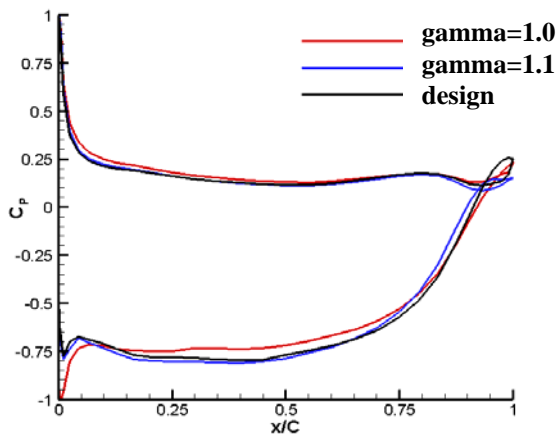


Figure 9. The pressure distributions corresponding to the designed foil and geometric parameters $\gamma = 1.0$ and $\gamma = 1.1$ in design example 3

3.3 Design Example 3

In the design example 3, we try to design a foil based on the given pressure distribution, but also to optimize its performance. In this example, we define the geometric parameter as a shape function of the pressure distribution. That is, we maintain the “shape” of the pressure distribution, and then scale it according to the geometric parameter γ . The design procedure is then as the following steps:

- (1) Giving a range of the geometric parameters γ to limit the designs, and in this case, $1.0 \leq \gamma \leq 1.1$;
- (2) For the initial γ , we have a pressure distribution, and a foil is designed according to this pressure distribution (equations (1) to (5));
- (3) Using the Lagrange Multiplier method to proceed the design. That is, to optimize the foil performance by updating the angle of attack α and the geometric parameter γ (equations (6) to (13));
- (4) For each geometric parameter γ , a new pressure distribution is obtained, and the step (2) is used to obtain the geometry generating this pressure distribution;
- (5) Repeat steps (3) and (4) until a convergent solution is obtained.

The given pressure distribution “shape function” of this design example is shown in Figure 7, along with the designed pressure distribution corresponding to $\gamma = 1.0$. A small negative pressure peak exists in the designed foil. The objective lift coefficient is set to be 0.76. When we adjust the geometric parameter, the suction side of the pressure distribution will be scaled (the lift is increased as the geometric parameter increases). The design results are shown in Table 3. By comparing to the lower and upper limits of the geometric parameters, we can find that the designed foil gives a lower drag coefficient. Figure 8 shows the designed foil geometry and geometries corresponding to $\gamma = 1.0$ and $\gamma = 1.1$. Figure 9 shows the pressure distributions corresponding to the designed foil and those corresponding to the geometric parameters $\gamma = 1.0$ and $\gamma = 1.1$.

Table 3 Design Results of the Design Example 3

	γ	α	C_L	C_D
Lower limit	1.000	2.94	0.76	0.00595
Upper limit	1.100	3.21	0.76	0.00845
Design	1.096	2.78	0.76	0.00474

4 INFLOW-ADAPTED FOIL DESIGN

A multi-objective inflow-adapted foil design will be demonstrated in this section. The design problem is described as follows:

- The design goal is to design a foil such that its performance is optimized at speed of 10 knots and 40 knots.

- The constraints are that the lift coefficient is 0.5 at 10 knots, and the lift coefficient has to be at least 0.4 at 40 knots.
- There are two geometric parameters, and the first geometric parameter γ_1 is selected as the chord-wise location (x/C) of the maximum camber ratio, and γ_1 is limited as $0.3 \leq \gamma_1 \leq 0.7$. The second geometric parameter γ_2 is the maximum camber ratio. The angle of attack is fixed at 0 degree.
- The objective is still to minimize the drag coefficient; however in order to equally compare the drag coefficients at different speeds, we normalize the drag coefficient by the drag coefficient of $\gamma_1 = 0.5$ foil (the maximum camber is at $x/C=0.5$), and the camber ratio is the value that satisfies $C_L^1 = 0.5$.
- The weighting function w are all selected as 0.5 ($w_1 = w_2 = 0.5$), that is, the performance at 10 knots and 40 knots are equally important.

This optimization problem thus can be stated as:

$$\begin{cases} \min & \tilde{C}_D^k & k=1,2 \\ \text{subject to} & \begin{cases} C_L^1 = 0.5 \\ C_L^2 \geq 0.4 \end{cases} \end{cases}$$

where \tilde{C}_D^k is the normalized drag coefficient.

In this design, the camber distribution is first defined at $\gamma_1 = 0.3$ and $\gamma_1 = 0.7$, and the $a=0.8$ mean-line is selected as the camber distribution corresponding to $\gamma_1 = 0.5$ (Figure 10). The camber distributions corresponding to different γ can be obtained by the interpolations among $\gamma_1 = 0.3$, $\gamma_1 = 0.5$ and $\gamma_1 = 0.7$. The thickness form is selected as a thickness distribution similar to the Eppler section thickness.

The computational tool is still the commercial RANS code FLUENT, and the cavitation is considered in the computations. Table 4 shows the designed geometric parameters and the performance comparing to the foil that $\gamma_1 = 0.5$. Figure 11 shows the designed foil geometry, and its pressure distribution at different speed at 0 degree angle of attack. From the pressure distributions shown in Figure 11, we know that the cavitation happens at 40 knots. Figure 12 shows the computed cavitation shape.

In order to investigate the global performance, we also make comparisons of the Bucket diagram and the lift to drag ratio between the designed foil and the $\gamma_1 = 0.5$ foil. Figure 13 shows the computed bucket diagram at speed of 40 knots, and one can see that, in terms of preventing cavitation, the $\gamma_1 = 0.5$ foil is better at lower cavitation numbers, and the designed foil is better at higher cavitation numbers. Figure 14 shows the computed lift to drag ratio at speed of 10 knots for different angles of attack, and Figure 15 shows the computed lift to drag ratio at speed of 40 knots. Apparently, the $\gamma_1 = 0.5$ foil has a better performance at 10 knots; however, the designed foil has a much better performance at 40 knots.

In this section, we have described the design of an inflow-adapted foil, and the camber distribution is selected as the geometric parameters. Other geometric parameters, such as the pressure distribution “shape function” as in section 3.3 can also be used. The different speeds is selected as the design conditions, and the different angles of attack can also be selected as the design conditions.

Table 4. The designed geometric parameters and the performance comparing to the $\gamma_1 = 0.5$ foil

	$\gamma_1 = 0.5$ foil	Designed foil
γ_1	0.5	0.655
Max. camber ratio	0.0981	0.0979
C_L at 10 knots	0.5	0.5
C_L at 40 knots	0.3819	0.4828
C_D at 10 knots	0.0088	0.0095
C_D at 40 knots	0.0402	0.0286

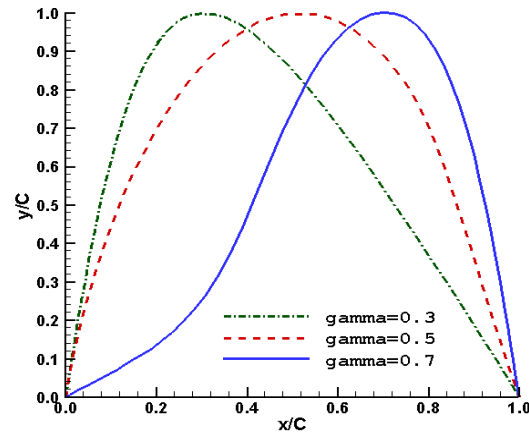


Figure 10. The camber distribution corresponding to geometric parameter $\gamma_1 = 0.3$, $\gamma_1 = 0.5$ and $\gamma_1 = 0.7$.

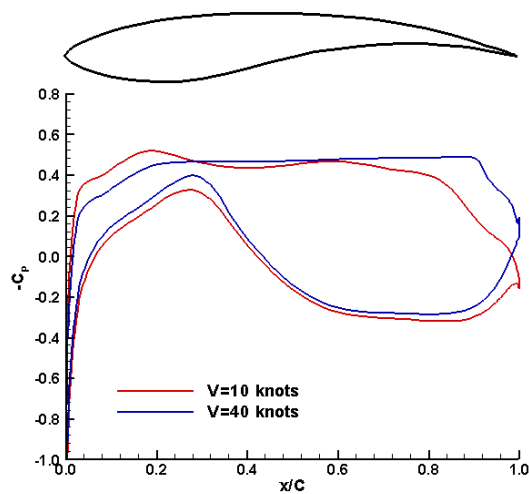


Figure 11. The designed foil geometry, and its pressure distribution at different speed at 0 degree angle of attack

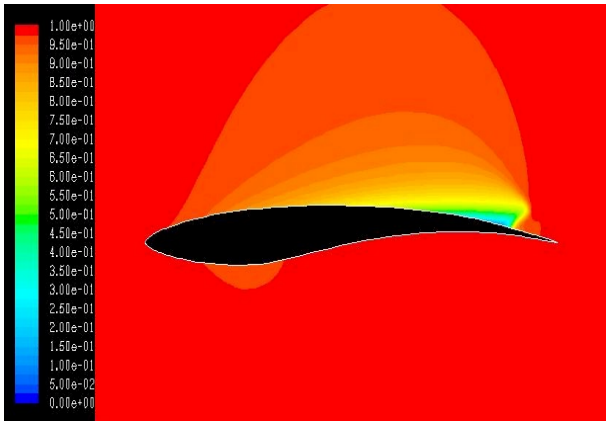


Figure 12. The computed cavitation shape for the designed foil at 40 knots and 0 degree angle of attack. The contour shows the volume fraction of water, and red color indicates 100% water.

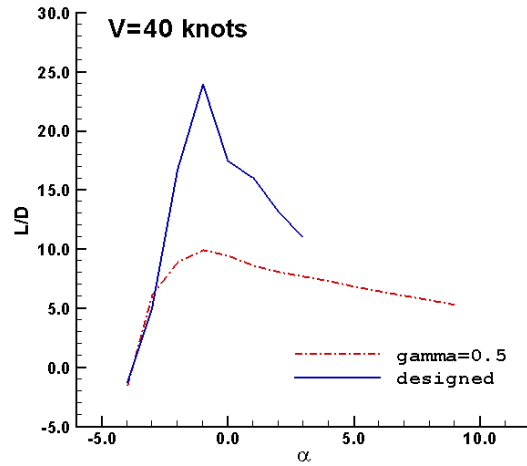


Figure 15. The computed lift to drag ratio at 40 knots

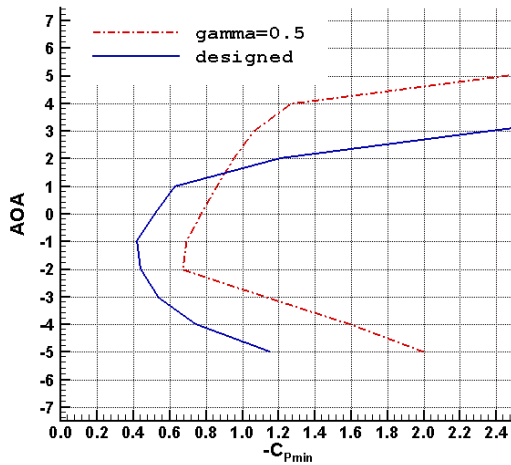


Figure 13. The computed bucket diagram for the designed foil and the $\gamma_1 = 0.5$ foil at 40 knots

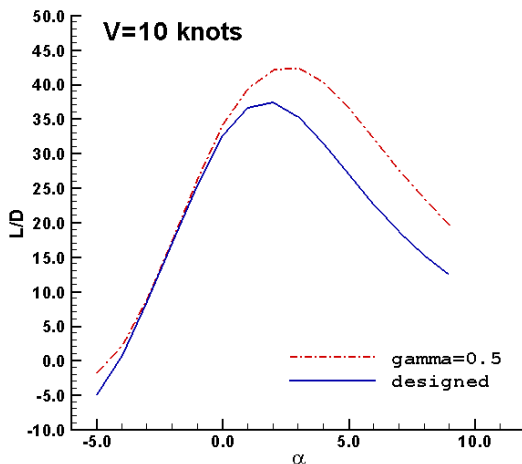


Figure 14. The computed lift to drag ratio at 10 knots

5 CONCLUSIONS

In this paper, a design procedure for designing the inflow-adapted foil is presented. Three design algorithms are described in the paper, and they are design a foil based on the given pressure distribution, single objective optimization method based on the Lagrange Multiplier method, and multi-objective optimization method based on the Lagrange Multiplier method. Design examples of single objective are shown in the paper, and a multi-objective inflow-adapted foil design is also presented. All the design cases show that the design method presented in this paper is effective. However, the designs are very time consuming due to using the viscous flow RANS method. A boundary element method with cavitation model and viscous correction may be more practical, and the RANS method can then be used to verify the final designs. A parametric design should also be carried out to compare the designs from the presented method.

The foil sections designed based on the presented procedure are expected to be used on propellers operated in a large range of speeds. If the multi-objective optimization is aimed to optimize the performance at different angles of attack, then the designed foil can be used for a propeller operated in an large inclined-shaft or a propeller in a severe wake. Nevertheless, more design cases are required to confirm the effectiveness of this design method.

REFERENCES

- De Falco., R. (1997). "An introduction to Evolutionary Algorithms and their application to the Aerofoil Design Problem Part I: The Algorithms", Inverse Design and Optimisation Method, von Karman Institute for Fluid Dynamics, Lecture Series
- De Falco. (1997). "An introduction to Evolutionary Algorithms and their application to the Aerofoil

- Design Problem Part II: The Results” , Inverse Design and Optimisation Method, von Karman Institute for Fluid Dynamics, Lecture Series
- Drela, M, (1989). “XFOIL: An Analysis and Design System for Low Reynolds Number Airfoils”, in Low Reynolds Number Aerodynamics, Vol. 54, Springer-Verlag Lecture Notes in Eng.
- Eppler, R. and Somers, D.M. (1980). “A Computer Program for the Design and Analysis of Low-Speed Airfoils”, Tech. Rep., NASA TM 80210
- Giles, M. Drela, M. (1986). “A two-dimensional transonic aerodynamic design method,” AIAA Journal, 25(9).
- Henne, P.A. (1985). “An inverse transonic wing design method”, AIAA paper 85-0330
- Hsin, C.-Y. (1994). "Application of the panel method to the design of two-dimensional foil sections", J. of Chinese Society of Naval Architecture and Marine Engineers, 13(2), pp.1-11.
- Hsin, C.-Y. and Chang, Y.-L. (1998). “Solving a Hydrodynamic Design Problem by a Distributed Computing System”, Proceedings of the 3rd International Conference on Hydro-dynamics, Seoul Korea.
- Hsin, C.-Y. and Chang, Y.-L. (2000). “A Hydrodynamic Design Method Developed on a Distributed Computing System”, Transactions of the Aeronautical and Astronautical Society, 32(1), pp.89-95.
- Lighthill, M.J. (1945) “A new method of two-dimensional aerodynamic design”, RAND Technical Report M2112, ARC.
- Obayashi S., Takanashi S. (1995) “Genetic Algorithm for Aerodynamic Inverse Optimization Problems,” Genetic Algorithms in Engineering Systems: Innovations and Applications, pp.7-12.
- Tranen, J.L. (1974) “A rapid computer aided transonic airfoil design method”, AIAA paper 74-501.
- Wu, J.-L. (2005) “Foil Design by Viscous Flow Computation,” Master Thesis, National Taiwan Ocean University (in Chinese)
- Volpe, G and Melnik, R.E. (1986). “The design of transonic airfoils by a well posed inverse method”, Int. J. Numerical Methods in Engineering, Vol. 22.